Multi-stability and variable stiffness of cellular solids designed based on origami patterns

Sattam Sengupta and Suyi Li[1]
Department of Mechanical Engineering, Clemson University, Clemson, SC 29634

ABSTRACT

The application of origami-inspired designs to engineered structures and materials has been a subject of much research efforts. These structures and materials, whose mechanical properties are directly related to the geometry of folding, are capable of achieving a host of unique adaptive functions. In this study, we investigate a three-dimensional multi-stability and variable stiffness function of a cellular solid based on the Miura-Ori folding pattern. The unit cell of such a solid, consisting of two stacked Miura-Ori sheets, can be elastically bistable due to the nonlinear relationship between rigid-folding deformation and crease material bending. Such a bistability possesses an unorthodox property: the critical, unstable configuration lies on the same side of two stable ones, so that two different force-deformation curves co-exist within the same range of deformation. By exploiting such unique stability properties, we can achieve a programmable stiffness change between the two elastically stable states, and the stiffness differences can be prescribed by tailoring the crease patterns of the cell. This paper presents a comprehensive parametric study revealing the correlations between such variable stiffness and various design parameters. The unique properties stemming from the bistability and design of such a unit cell can be advanced further by assembling them into a solid which can be capable of shape morphing and programmable mechanical properties.

Keywords: Miura-ori, bistability, programmable stiffness, variable elastic moduli

1. INTRODUCTION

Origami – developed in the early 1600s – is a Japanese craftsman art of folding paper into decorative shapes and geometries[1]. Originally it was used primarily for recreational and artistic purposes; however, over the past several decades, progress in the mathematical theories of paper folding has led to the emergence of origami inspired architectural and engineering applications. One such engineering application that was exploited early is the use of foldable solar panels on spacecraft. Koryo Miura designed a folding pattern for the solar panels so that they can be folded to fit in the confined space of launch vehicles and then deployed after the spacecraft reaches its orbit[2]. This folding pattern design was subsequently named as the Miura-*ori* (Fig. 1a). This pattern tessellates the surface into a grid of parallelogram facets connected via either valley and mountain creases. Miura-*ori* pattern is rigid-foldable, meaning that it can fold smoothly even if the facets are rigid and creases behave like hinges, so that its folding is essentially a one degree of freedom mechanism. Therefore, once the Miura-*ori* is folded, a single actuation force can be used to fold or unfold the whole structure.

Recent researches have shown that the Miura-*ori* sheets can also become the building blocks of architectured structures and materials. Especially, the Miura-*ori* and its close relatives, such as the single-collinear pattern, have translational periodic morphologies so that they can be stacked and connected to form a three dimensional cellular solid, whose mechanical properties are dictated by the kinematics of folding (Fig. 1b,c). The intricate and nonlinear

[1] Further author information (send correspondence to Suyi Li)
Sattam Sengupta Email: ssengup@g.clemson.edu
Suyi Li Email: suyil@clemson.edu

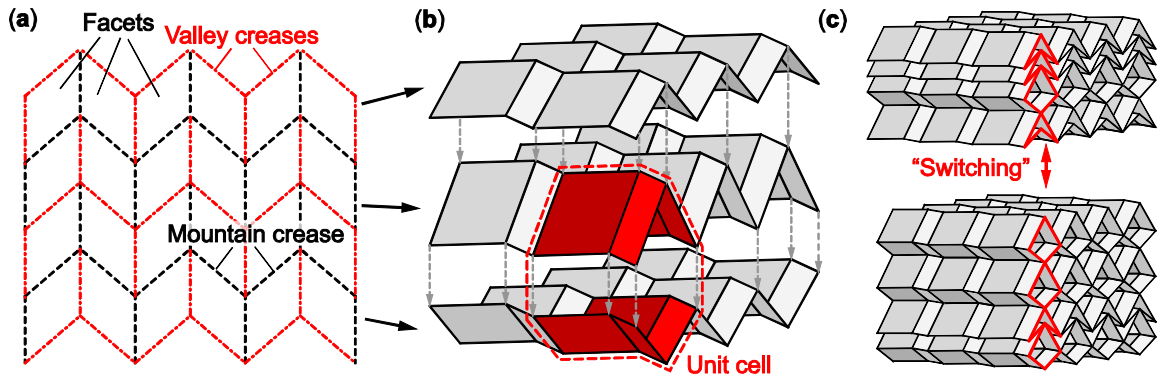

Figure 1. The concept of stacking Miura-*ori* sheets into a cellular solid. (a) The pattern design of Miura-*ori*, consisting of parallelogram facets connected by mountain or valley folds. (b) Folded Miura-*ori* sheets can be stacked and connected along their creases. A unit cell is highlighted. (c) The stacked Miura can fold to different configurations, each features unique mechanical properties.

correlations between folding and external deformations can impart some unique and programmable mechanical properties to the stacked origami solid, such as negative Poisson's ratio[3–5], self-locking and discrete stiffness jumps[6], and elastic multi-stability[7–11]. Among them the multi-stability is particularly appealing because it can serve as a catalyst for a wide variety of adaptive functionalities including shape morphing and impulsive actuation[12], stiffness adaptation[13,14], vibration management and energy harvesting[15–17]. In the stacked Miura-*ori*, multi-stability can occur when the crease bending stiffness between adjacent origami sheets are significantly different, so that the overall structure can possess multiple stable states with distinct internal folding configurations (Fig. 1c). The stacked Miura-*ori* can settle into one of these stable states without any aids, and can be 'switched' between them via external actuations. Compared to other previously investigated multi-stable mechanisms such as the curved beams and pre-stressed composite plates with asymmetric laminate layout[12], the stacked origami is unique in that its shape transformation via folding is fundamentally three dimensional, which can be harnessed to achieve adaptive functions that are unavailable from the lower-dimensional mechanisms.

This research examines the variable stiffness function of stacked origami solid by switching between its different stable states. To investigate the underlying physical principles without unnecessary complexities, this study focuses on a unit cell in the cellular solid, which consists of two kinematically compatible Miura-*ori* sheets stacked on top of each other (Fig. 1b). With appropriate designs, such a unit cell can possess two stable configurations and thus deemed bistable. The fundamentally three-dimensional nature of origami folding creates a unique bistable properties that are never reported before in the lower-dimensional bistable mechanisms: Along certain principle orientations, the two stable states of the origami unit cell lie on the same side of the critical, unstable configuration. Such unorthodox property makes the unit cell appear *almost mono-stable* within the majority of its deformation range, and within this range, two distinct reaction force curves exist concurrently. These two force-deformation curves feature different stiffness values, which makes it possible for the stacked origami to exhibit variable stiffness via switching between the stable configurations. Furthermore, the magnitudes of the stiffness along the two force-deformation curves can be programmed by tailoring the key design parameters with a large performance space. Therefore, a large scale stacked origami solid consisting of many unit cells has the potential of switching between different prescribed stiffness (or elastic moduli) on-demand. All of these unique variable stiffness properties, together with the ease of fabrication of such structures (e.g. via 3D printing), can potentially lead to novel adaptive structure and materials with attractive application appeals such as morphing structures[18] and soft robotics[19].

The objective of the work presented in this paper is to uncover the physical principles behind the folding-induced variable stiffness and its correlations to the Miura-*ori* design. The rest of this paper is organized as follows: Section 2 discusses the design and folding kinematics of the Miura-*ori* unit cell and the associated constraints from stacking. Section 3 examines how this unit cell achieves the unique bistability and variable stiffness. Section 4 identifies the key design parameters which control the range of bistability and also affect the values of stiffness ratio. Section 5 concludes this paper with summary and discussions.

2. GEOMETRY AND KINEMATICS OF FOLDING

A unit Miura cell is formed when two Miura-*ori* sheets are stacked on top of each other and connected along their crease lines (Fig. 1b, 2). Such a unit cell is the most elementary unit for achieving multi-stability, and its elastic characteristics are representative to the overall stacked origami solid. Especially, the results can be extended to the entire solid if all unit cells are assumed identical. This study assumes the Miura sheets are rigid origami, meaning that the facet materials are rigid and the creases act like hinges with some torsional stiffness. The geometric parameters that define a Miura cell are the lengths of two adjacent edges of a facet (a_k and b_k in Fig. 2a) and the sector angle between these two edges (γ_k). These parameters remain constant over the entire folding range of the cell. The subscripts k (=I, or II) denotes the two different Miura sheets in a unit cell. In this paper, the Miura sheet with the shorter crease is denoted by 'I'. The folding motion of the cell is defined by the dihedral folding angle (θ_I) defined between the facets and *x*-*y* reference plane. There are three design constraints which the two Miura sheets have to satisfy so that they are kinematically compatible and stay connected throughout their entire range of folding[3]:

$$b_\mathrm{II} = b_\mathrm{I}, \tag{1}$$

$$\frac{\cos\gamma_\mathrm{II}}{\cos\gamma_\mathrm{I}} = \frac{a_\mathrm{I}}{a_\mathrm{II}}, \tag{2}$$

$$\frac{\cos\theta_\mathrm{II}}{\cos\theta_\mathrm{I}} = \frac{\tan\gamma_\mathrm{I}}{\tan\gamma_\mathrm{II}}. \tag{3}$$

The folding angle θ_I of the Miura sheets I varies from -90° to 90° (Fig. 2). Since θ_I and θ_II are kinematically constrained according to the aforementioned relations, folding of the unit cell is still a one degree of freedom mechanism. Therefore, the folding angle of sheet I (θ_I) is chosen as the independent variable and from henceforward is denoted simply by θ. Over the folding range of the unit cell, its external dimensions along the *x*-, *y*- and *z*- coordinates (i.e. the length, width and height) are defined as a function of the folding angle θ [11].

$$L = 2b_\mathrm{I}\cos\theta\tan\gamma_\mathrm{I}\left(1+\cos^2\theta\tan^2\gamma_\mathrm{I}\right)^{-1}, \tag{4}$$

$$W = 2a_\mathrm{I}\sqrt{1-\sin^2\theta\sin^2\gamma_\mathrm{I}}, \tag{5}$$

$$H = a_\mathrm{I}\sin\gamma_\mathrm{I}\left(\sqrt{\frac{\tan^2\gamma_\mathrm{II}}{\tan^2\gamma_\mathrm{I}}-\cos^2\theta}-\sin\theta\right). \tag{6}$$

Figure 2(c) illustrates the external dimensions of the Miura cell over its entire folding range, and the corresponding design parameters are summarized in Table 1. Unless otherwise noted, results of the rest of this paper are based on the sample designs in this table. The relationship between the unit cell height (*H* along the z-axis) and the

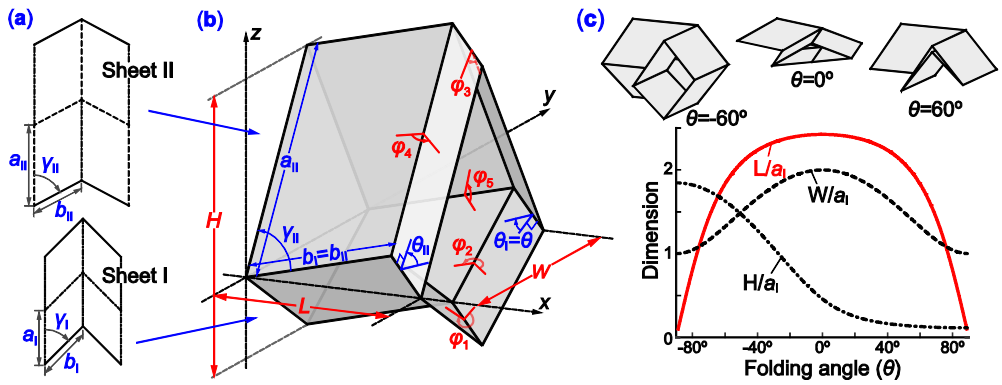

Figure 2. Geometry and folding kinematics of a unit Miura cell. (a) Geometric design parameters of the Miura-*ori*. (b) The external dimension (L, W, H), folding angles (θ_{I}, θ_{II}) and dihedral angle (φ_i) of the unit cell. (c) The changes in external dimensions with respect to folding. Note that the relationship between height and sheet I folding angle is monotonic, while those between length/width and folding are not.

folding angle (θ) is monotonic, however, the mappings between the unit cell length (L), width (W) and the folding angle are not. That is, as the folding angle increases from -90° to 90°, both L and W will increase first until they reach the maximum values at $\theta = 0$, and then decrease. Such strongly nonlinear co-relationships between folding and external deformations play the central role for the unorthodox bistability properties discussed in the following section. When the unit cell is folded, there exists five unique dihedral angles between adjacent facets (Fig. 2)[11],

$$\varphi_1 = \pi - 2\theta, \tag{7}$$

$$\varphi_2 = 2\sin^{-1}\left(\frac{\cos\theta}{\sqrt{1-\sin^2\theta\sin^2\gamma_{\mathrm{I}}}}\right), \tag{8}$$

$$\varphi_3 = \pi - 2\cos^{-1}\left(\tan\gamma_{\mathrm{II}}\tan^{-1}\gamma_{\mathrm{I}}\cos\theta\right), \tag{9}$$

$$\varphi_4 = 2\sin^{-1}\left(\frac{\sin\gamma_{\mathrm{I}}}{\sin\gamma_{\mathrm{II}}}\sin\frac{\varphi_2}{2}\right), \tag{10}$$

$$\varphi_5 = \cos^{-1}\left(\tan\gamma_{\mathrm{II}}\tan^{-1}\gamma_{\mathrm{I}}\cos\theta\right) - \theta. \tag{11}$$

Since the facets are assumed rigid, folding motion of Miura-*ori* are concentrated on the crease lines, which bend according to dihedral angles defined in Eq. (7-11). To characterize the stiffness associated to folding, one can assign torsional spring stiffness *per unit length* to the creases in the unit cell. Denote k_{I} and k_{II} as the crease spring stiffness per unit length of sheet I and II, respectively, and k_c as the stiffness per length of the creases shared by the two Miura sheets. The torsional spring constants corresponding to the unique dihedral angles in Eq. (7-11) can be defined as $K_1 = 2k_{\mathrm{I}}b$, $K_2 = 2k_{\mathrm{I}}a_{\mathrm{I}}$, $K_3 = 2k_{\mathrm{II}}b$, $K_4 = 2k_{\mathrm{II}}a_{\mathrm{II}}$, and $K_5 = 4k_c b$, where the numerical values in these equations are the number of creases that have the same dihedral angle. Therefore, the total elastic energy from folding is a summation from those of individual creases[11]:

$$E = \frac{1}{2}\sum_{i=1}^{5} K_i \left(\varphi_i - \varphi_i^{\circ}\right)^2, \tag{12}$$

where φ_i° are the dihedral angles corresponding to a stress-free folding angle (θ°), where no creases are subjected to any bending deformation.

Table 1. Sample Miura unit cell design parameters

Geometric parameter	Value	Material parameter	Value
a_{I}	25 mm	k_{I}	5 N
a_{II}	27.5 mm	k_{II}	50 N
b	35 mm	k_c	5 N
γ_{I}	60°		
θ°	-60°		

3. BISTABILITY AND VARIABLE STIFFNESS OF UNIT CELL

Figure 3 illustrates the energy landscape of a unit Miura cell with respect to its sheet I folding angle (θ) based on the sample set of design parameters shown in Table 1. The double potential energy wells, which are the defining characteristics of a bistable system, are evident based on this design. Generally speaking, bistability is easier to achieve when the crease stiffness of sheet II (k_{II}) is significantly bigger than those of sheet I (k_{I}), or the stress-free folding angle (θ°) deviate away from 0°. For clarity, the stable state where the sheet I is folded out ($\theta < 0$) is designated to as the '+' configuration and the other folded in configuration ($\theta > 0$) is designated as the '-' configuration. The critical, elastically unstable state is designated as the 'o' configuration.

The energy landscape in Fig. 3 are calculated with respect to the folding angle, however, it is necessary to calculate the energy with respect to the unit cell deformation in order to investigate its stiffness. Figure 4(a, b) illustrate the energy landscapes with respect to the height and length of the unit cell, which are calculated by combining Eq. (4 -6) and (12). And the corresponding reaction force (F_j) can be calculated via virtual work principle (Fig.4c,d):

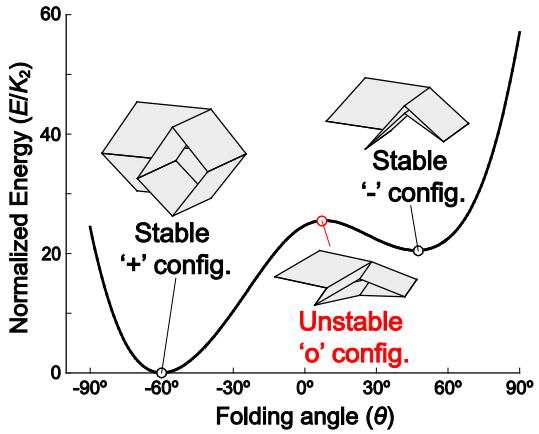

Figure 3. The total potential energy of the unit Miura cell plotted over its entire folding range. The two 'wells' in the curve are the stable configurations. For this particular design (shown in Table 1), the '+' configuration has a folding angle of -60°, which is exactly the stress-free folding angle (θ°). The '-' configuration has $\theta = 47^{\circ}$; and the unstable, 'o' configuration has $\theta = 8^{\circ}$.

$$F_j = \frac{\partial E}{\partial X} = \frac{\partial E}{\partial \theta}\left(\frac{\partial X}{\partial \theta}\right)^{-1}, \quad X = H \text{ or } L. \tag{13}$$

Along the height direction (z-axis in Fig. 2), the elastic unstable state of the unit cell locates between the two stable ones; and the corresponding force deformation curve consists of two segments with positive slopes (aka. positive stiffness) connected by a segment with negative slopes between them (Fig. 4a,c). These characteristics are the results of the monotonic relationship between unit cell height and folding angle (Fig. 2d), and they are very similar to many other bistable mechanisms such as the curved bistable beams and asymmetric composite laminates. Therefore, applying a sufficiently large external force along this axis can switch the cell between the two stable states (dashed arrow in Fig. 4c). However, along the x-axis (length direction), the unstable state is located on the same side of the two stable ones due to the non-monotonic relationship between folding and external deformation (Fig. 2b). In addition, this unstable state can be very close to the maximum length allowed by rigid-folding (aka. rigid facets and hinge-like crease lines). As a result, the unit cell *appears mono-stable* over the majority of its deformation range with respect to the external forces along x-axis (grey region in Fig. 4d). Switching between the two stable states will not occur unless the origami is stretched almost to the maximum where the elastic instability occurs ('o' in Fig. 4). Similar characteristics were also available in the y-axis (width direction).

Such an unorthodox distribution of elastic equilibria in the unit Miura cell can be harnessed to achieve variable stiffness. Within the deformation range in which a unit cell appears mono-stable, two different force-deformation curves coexist, which means that the unit cell can exhibit two different nonlinear stiffness along the x and y-axes. And the unit cell can be switched between the two force deformation curves via a control force along the z-axis, or via internal pressurization[11]. Although variable stiffness from bistability were investigated in other structures before[18], the stacked origami has unique advantages. First of all, since deformation range of the two force-deformation curves overlap, it is possible to switch to different stiffness level with minimal change in external dimension. Secondly, the critical, unstable equilibrium occurs near the maximum length or width, which can reduce the possibility of unwanted snap-through. To examine the variable stiffness and its correlation to the origami design, in this paper we particularly focus on the tangent stiffness at the two stable configurations along the x (length) axis, denoted as K_+ and K_-, respectively (Fig. 4d). The magnitudes of these stiffness are calculated as the second order derivative of the elastic energy curve with respect to the change in length. The to-scale plots of the unit cell at the two stable configuration in Fig. 3 reveals that the stiffness difference between the two stable states originates from the changes in spatial locations of the linearly elastic creases.

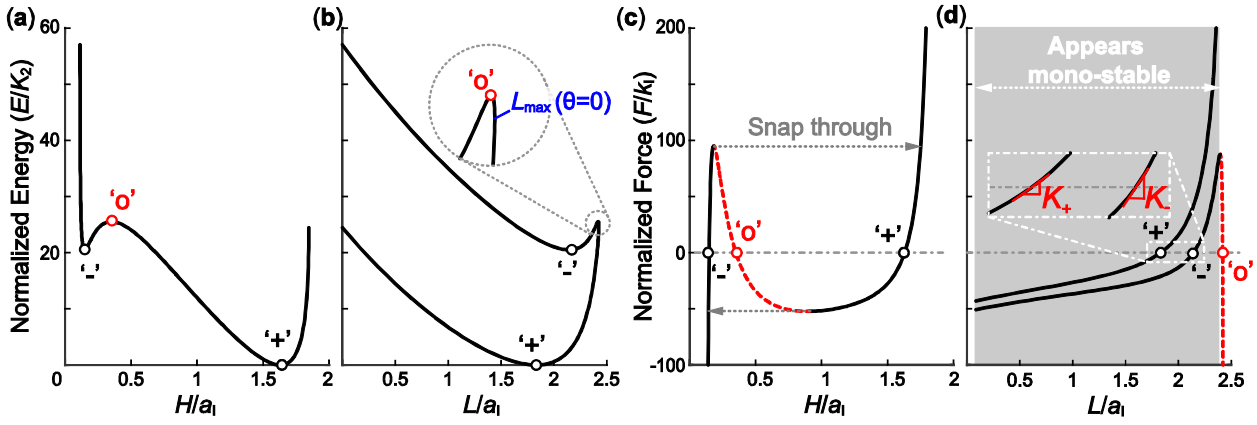

Figure 4. The energy landscape (a, b) and corresponding reaction force (c, d) of the unit cell with respect to external deformation in height (a, c) and length (b, d). The two co-existing force-deformation curves corresponding to the two stable states are evident in (d). K_+ and K_- are defined as the tangent stiffness along length direction at the state states. The dashed segments in the reaction force curves corresponds to negative stiffness region.

4. IDENTIFYING KEY DESIGN PARAMETERS

One unique feature of the stacked origami is that its bistability and variable stiffness can be prescribed with a large freedom by tailoring the design parameters of the constituent Miura-*ori* sheets. In order to establish a comprehensive design framework for the variable stiffness, a parametric study was carried out to identify the key design parameters. The aim of this parametric study was to examine which parameters can mostly affect the *stiffness ratio* between the two stable configurations, defined as K_-/K_+. Two groups of design parameters are investigated, the first group are geometric parameters of the two Miura-*ori* sheets, including the crease length (a_k, b_k, k = I, II), sector angles (γ_k), and stress-free folding angle (θ^o). The second group are material parameters, including the crease torsional stiffness per unit length (k_I, k_II). For each parametric study, one parameter is varied while all others remain constant based on the example designs in Table 1.

Parametric analyses revealed that the ratios of between crease lengths affect the stiffness ratio more than the actual lengths themselves. Therefore, for ease of calculations, a_I was held constant, and a_II, b were varied as a ratio to a_I. Analyses showed that changes in the normalized geometric parameters ($a_\mathrm{II}/a_\mathrm{I}$, b/a_I, and γ_I) affect the stiffness ratio the most, thus they are designated as the key design parameters. On the other hand, changing the material parameters (k_I, k_II) had relatively smaller effects on stiffness ratio; moreover these material parameters are more difficult to be tailored compared to the geometric ones. Therefore, they are designated as the secondary design parameters. Figure 5 shows the correlation between the stiffness ratio (K_-/K_+) and the key design parameters.

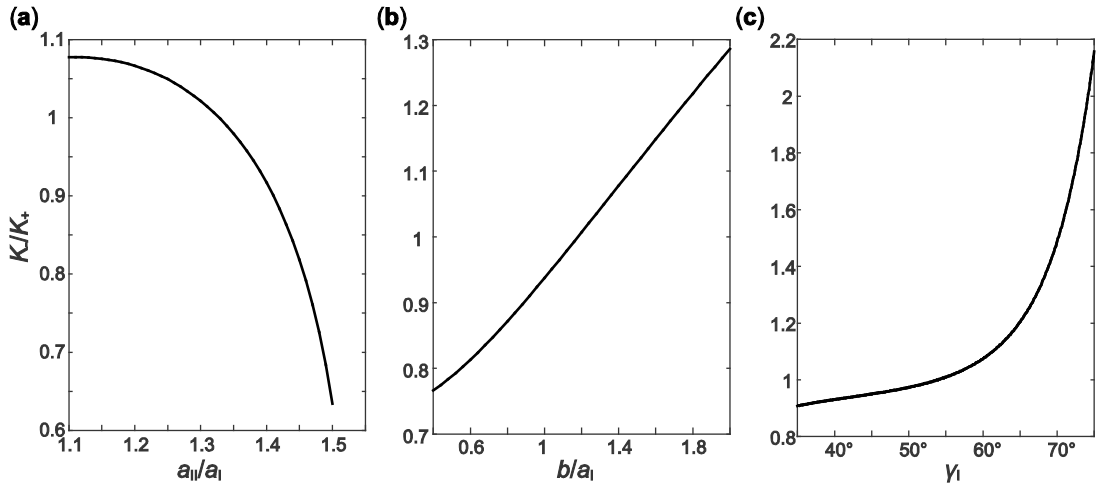

Figure 5. The correlation between the normalized design parameters and the stiffness ratio (K_-/K_+). The key design parameters are (a) $a_\mathrm{II}/a_\mathrm{I}$, (b) b/a_I, and (c) $\gamma_\mathrm{I}/a_\mathrm{I}$.

5. VARIABLE STIFFNESS PERFORMANCE SPACE

Once the key design parameters are identified, one can further explore the performance space of the variable stiffness from stacked origami. For example, two key parameters can be varied simultaneously and their effects on the stiffness ratio can be mapped out in contour plots in Fig. 6. These contour plots can establish a design framework by which one can choose suitable parameters to achieve targeted stiffness ratio. Moreover, the range of bistability of the unit Miura cell can also be investigated, because the contour plots can precisely reveal the combination of design parameters that makes the unit cell mono-stable (white region in Fig. 6). It is interesting to note that the magnitude of K_-/K_+ can becomes less than one in a narrow band of design space close to the mono-stability region. This

indicates that either of the two stable configuration can possess a higher magnitude of stiffness depending on the Miura-*ori* design.

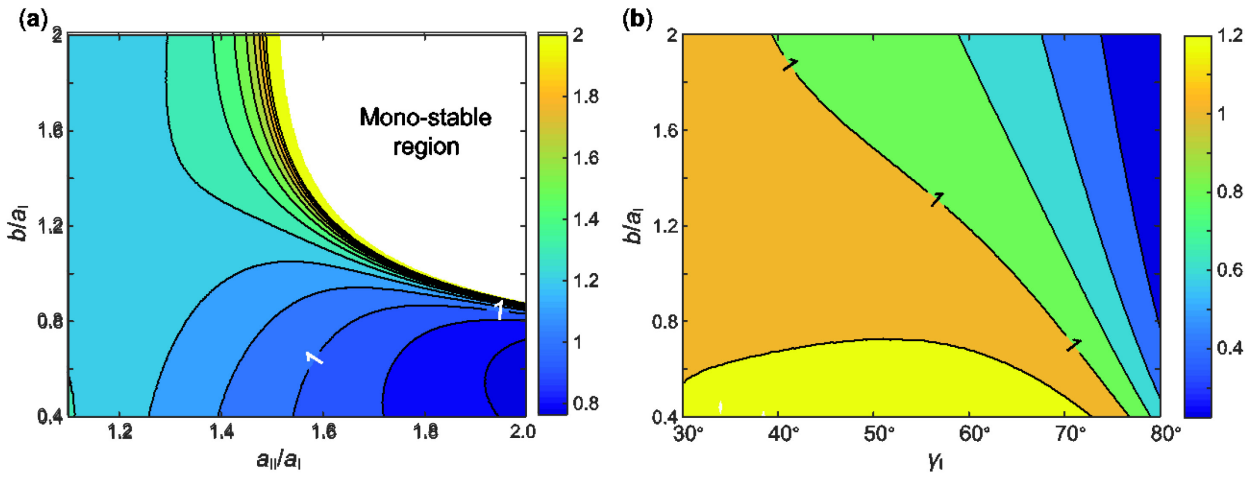

Figure 6. The effect on the stiffness ratio K_-/K_+ when the interaction of the key parameters is considered. The unshaded region depicts the designs that leads to mono-stability. The contour line of $K_-/K_+ = 1$ marks the crossing over where the stiffness magnitude of the '+' configuration becomes higher than that of the '-' configuration.

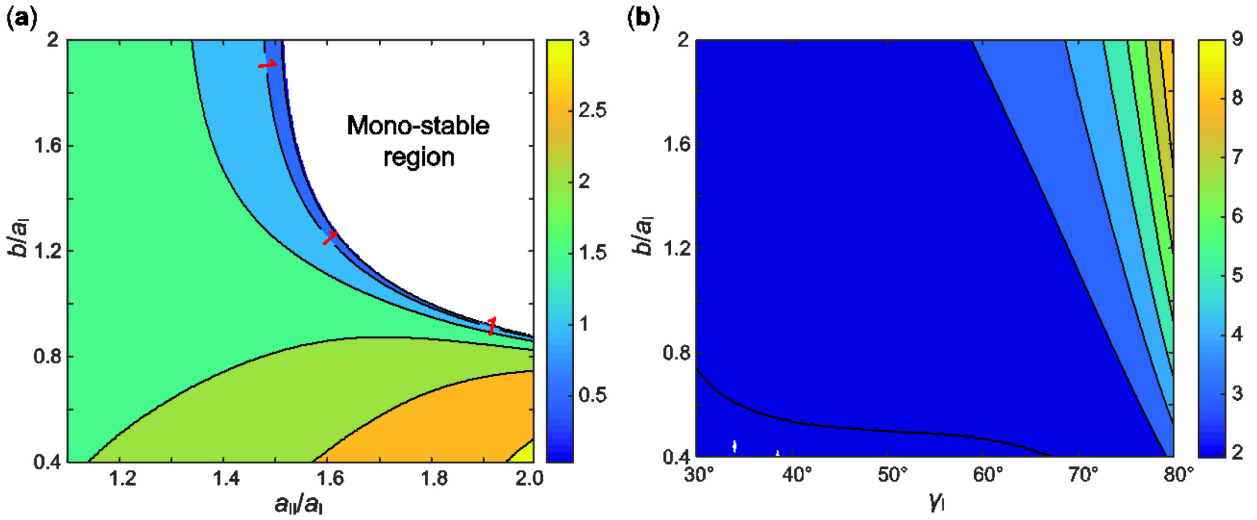

Figure 7. The interaction of the design parameters also shows their effect on the E_-/E_+, ratio. The overall effective modulus of a Miura solid can be varied by selecting a desired performance output and the parameters can be tweaked to achieve the set output.

Since the unit Miura cell is intended as most elementary unit of the large scale stacked origami solid (Fig. 1), it is necessary to translate the variable stiffness results into equivalent variable elastic modulus. Assuming all of the unit cells in the stacked cellular solid are identical in terms of their geometric and material designs as well as folding configurations. The effective elastic modulus of the stacked origami, along the length direction (*x*-axis), can be calculated based on the unit cell as $E = 2(K_x L)/(WH)$, where K_x is the unit cell stiffness along x-axis and *L*, *W*, *H* is the external dimensions defined in Eq. (4-6). A set of contour plots for the variable elastic modulus are shown in

Figure 7. The color bar in this figure represents the ratio of E_-/E_+, where E_+ and E_- are the effective elastic moduli at the '+' and '-' stable configurations, respectively. A wide range of the modulus ratio (from less than 0.5 to 10) can be observed within the design parameter range shown in Fig. 7.

It is worth noting that the elastic modulus calculations in Fig. 7 assume that all of the unit cells in the stacked origami solid are settled in the same stable state, that is, all of them are either in the '+' configuration or the '-' one. However, the kinematics of rigid folding allows the unit cells to settle in different stable states, therefore, a stacked solid with a large number of unit cells can exhibit more than two levels of elastic moduli. Individually switching the unit cells between '+' and '-' configurations can open up the avenue towards programming the stiffness of the cellular materials or structures on demand. Investigating such stiffness programming from the large scale cellular solid is beyond the scope of this paper, and it is a worthy subject of future research.

6. SUMMARY AND CONCLUSION

This study aims to examine the elastic multi-stability of a stacked origami solid and how it can impart a variable stiffness function. In particular, this work focuses on an elementary unit cell consisting of two different Miura-*ori* sheets to uncover the underlying physical principles. This unit cell can be elastically bistable due to the non-linear relationships between the rigid-folding deformation and the crease material bending. The bistability is unique and differs from the previously investigated bistable mechanisms because the deformation via folding is fundamentally three-dimensional. As a result, along the length and width directions of the unit cell, the critical, unstable equilibrium occurs at the same side of the two stable ones rather than in between them. Such unorthodox arrangement of the equilibria can be harnessed to achieve a variable stiffness function, because the Miura cell can exhibit different stiffness between the two stable states, and the deformation range corresponding to these two stable states overlap. A unique feature of the stacked origami is that the variable stiffness performance can be prescribed by tailoring the designs of the constituent Miura-*ori* sheets. Thus a parametric analysis is carried out to identify the key design parameters. It is found that changing the geometric design parameters, such as the length ratio between crease lines and sector angle, can significantly influence the variable stiffness ratio. Therefore, one can leverage such relationships between the origami design and variable stiffness to create cellular structures and materials that can be switched to different stiffness properties on demand. Results of this study have the potential of advancing the start of the art of many adaptive systems, such as morphing structures and soft robotics.

7. ACKNOWLEDGEMENT

The authors acknowledge the support by the National Science Foundation (award # CMMI-1633952) and the startup funding from Clemson University.

REFERENCES

[1] McArthur, M., Lang, R. J., Folding Paper: The Infinite Possibilities of Origami, 1sted., Tuttle Publishing, Rutland, VT, USA (2013).

[2] Nishiyama, Y., "Miura folding: applying origami to space exploration," Int. J. Pure Appl. Math. **79**(2), 269–279 (2012).

[3] Schenk, M., Guest, S. D., "Geometry of Miura-folded metamaterials," Proc. Natl. Acad. Sci. **110**(9), 3276–3281 (2013).

[4] Eidini, M., Paulino, G. H., "Unraveling metamaterial properties in zigzag-base folded sheets," Sci. Adv. **1**(8), e1500224 (2015).

[5] Fang, H., Li, S., Ji, H., Wang, K. W., "Uncovering the deformation mechanisms of origami metamaterials by introducing generic degree-four vertices," Phys. Rev. E **94**(4), 43002 (2016).
[6] Fang, H., Li, S., Wang, K. W., "Self-locking degree-4 vertex origami structures," Proc. R. Soc. A Math. Phys. Eng. Sci. **472**(2195), 20160682 (2016).
[7] Waitukaitis, S., Menaut, R., Chen, B. G., van Hecke, M., "Origami multistability: from single vertices to metasheets," Phys. Rev. Lett. **114**(5), 55503 (2015).
[8] Silverberg, J. L., Na, J. H., Evans, A. A., Liu, B., Hull, T. C., Santangelo, C. D., Lang, R. J., Hayward, R. C., Cohen, I., "Origami structures with a critical transition to bistability arising from hidden degrees of freedom," Nat. Mater. **14**(4), 389–393 (2015).
[9] Hanna, B. H., Lund, J. M., Lang, R. J., Magleby, S. P., Howell, L. L., "Waterbomb base: a symmetric single-vertex bistable origami mechanism," Smart Mater. Struct. **23**(9), 94009 (2014).
[10] Cai, J., Deng, X., Ya, Z., Jiang, F., Tu, Y., "Bistable behavior of the cylindrical origami structure with Kresling pattern," J. Mech. Des. **137**(6), 61406 (2015).
[11] Li, S., Wang, K. W., "Fluidic origami with embedded pressure dependent multi-stability : a plant inspired innovation," J. R. Soc. Interface **12**(111), 20150639 (2015).
[12] Emam, S. A., Inman, D. J., "A review on bistable composite laminates for morphing and energy harvesting," Appl. Mech. Rev. **67**(6), 60803 (2015).
[13] Harne, R. L., Wu, Z., Wang, K. W., "Designing and Harnessing the Metastable States of a Modular Metastructure for Programmable Mechanical Properties Adaptation," J. Mech. Des. **138**(2), 21402, American Society of Mechanical Engineers (2015).
[14] Florijn, B., Coulais, C., van Hecke, M., "Programmable mechanical metamaterials," Phys. Rev. Lett. **113**(17), 175503 (2014).
[15] Pellegrini, S. P., Tolou, N., Schenk, M., Herder, J. L., "Bistable vibration energy harvesters: A review," J. Intell. Mater. Syst. Struct. **24**(11), 1303–1312 (2013).
[16] Harne, R. L., Wang, K. W., "A review of the recent research on vibration energy harvesting via bistable systems," Smart Mater. Struct. **22**(2), 23001 (2013).
[17] Daqaq, M. F., Masana, R., Erturk, A., Dane Quinn, D., "On the role of nonlinearities in vibratory energy harvesting: A critical review and discussion," Appl. Mech. Rev. **66**(4), 40801 (2014).
[18] Kuder, I. K., Arrieta, A. F., Raither, W. E., Ermanni, P., "Variable stiffness material and structural concepts for morphing applications," Prog. Aerosp. Sci. **63**, 33–55 (2013).
[19] Manti, M., Cacucciolo, V., Cianchetti, M., "Stiffening in soft robotics: A review of the state of the art," IEEE Robot. Autom. Mag. **23**(3), 93–106 (2016).